Hindawi
International Journal of Rotating Machinery
Volume 2021, Article ID 6684329, 16 pages
https://doi.org/10.1155/2021/6684329

Research Article

Experimental Investigations on Leakages in Positive Displacement Machines

Hitesh H. Patel[1,2] **and Vikas J. Lakhera**[1]

[1]*Department of Mechanical Engineering, Institute of Technology, Nirma University, -382481, Ahmedabad, India*
[2]*Engineering Department-Compressor Technologies and Services, Ingersoll Rand (I) Limited, -382330, Ahmedabad, India*

Correspondence should be addressed to Vikas J. Lakhera; vikas.lakhera@nirmauni.ac.in

Received 4 December 2020; Accepted 7 August 2021; Published 21 August 2021

Academic Editor: M. Razi Nalim

The clearance gaps in positive displacement machines such as compressors, pumps, expanders, and turbines are critical for their performance and reliability. The leakage flow through these clearances influences the volumetric and adiabatic efficiencies of the machines. The extent of the leakage flow depends on the size and shape of clearance paths and pressure differences across these paths. Usually, the mass flow through the gaps is estimated using the isentropic nozzle equation with the flow coefficients applied to correct for the real flow conditions. However, the flow coefficients applied generally do not take into account the shape and size of these leakage paths. For that reason, a proper understanding of the relationship between flow coefficients and shape parameters is crucial for an accurate prediction of leakage flows. The present study investigates the influence of the various dimensionless parameters such as Reynolds number, Mach number, and pressure ratio on the flow coefficients for circular and rectangular clearance shapes. The flow coefficients are determined by comparing the experimental values obtained in an experimental test rig and the flow rates obtained from the isentropic nozzle equation. It is observed that in the case of circular clearances, the mean deviation of the experimental leakage results (in comparison to the analytical results using isotropic nozzle equations) is +9.1%, which is significantly lower than the mean deviation (+20.5%) in the case of rectangular clearance leakages. The study indicates that the isentropic nozzle equation method is more suitable for predicting the leakages through the circular clearances and needs modifications for consideration of the rectangular clearances. Using regression analysis, empirical correlations are developed to predict the flow coefficient in terms of Reynolds number, Mach number, pressure ratio, aspect ratio, and β ratio, which are found to match within ±6.4 percent of the numerical results for the rectangular clearance and within the range of -3.6 percent to +5.1 percent of the numerical result for the circular clearance. The empirical relationships presented in this study can be extended to evaluate the flow coefficients in a positive displacement machine.

1. Introduction

The positive displacement machines such as screw machines, scroll machines, vane machines, root blowers, and piston-cylinder machines are widely used in the industry for a variety of applications. Among all the industrial products, electrical motors and electrical motor-driven systems (EMDS) have more focus, as they consume almost half of the total electricity used in the industry. It has more potential (20% to 30%) to improve the energy efficiency of the systems and reduce the total global electricity consumption by about 10% [1]. That is the reason many countries have introduced mandatory and voluntary measures of efficiency for motor-driven products, which also include positive displacement machines. The optimal design of positive displacement machines results in higher efficiencies, lower operating cost, and a more sustainable product.

The clearance gaps in positive displacement machines are critical for their performance and reliability. The leakage flow through these clearances influences the volumetric and

Table 1: Leakages in positive displacement machines.

Type of machine	Applications	Parts (which creates clearance paths)	Type of leakages	Simplified clearance structure
Reciprocating machines [2, 3]	Compression, pumping, expansion	Piston and cylinder	Piston-cylinder clearance leakages Valve and valve plate seat clearance leakage	Annular Circular
Screw machines [4]	Compression, pumping, expansion	Rotors and housing	Interlobe leakages Rotor-tip housing leakages End plate leakages Blowhole leakages	Rectangular Triangular
Vane machines [5]	Compression, pumping, expansion	Rotor, rotor blades, and housing	Radial leakages End plate leakages Leakages from isolated volumes	Rectangular
Claw (rotary tooth) machines [6]	Compression and pumping	Rotors and housing	Leakages from isolated volumes End plate leakages Tip and housing leakages	Rectangular
Root blowers [7]	Compression, pumping, expansion	Roots lobe and housing	Interlobe leakages Lobe-tip housing leakages End plate leakages	Rectangular
Scroll machines [8]	Compression, pumping, expansion	Fixed scroll and orbiting scroll	Tip seal leakages (tangential and radial leakage)	Rectangular
Rotary valves [9]	Multiple applications	Impeller and housing	Axial clearance leakages Radial clearance leakages	Rectangular

adiabatic efficiencies of the machines. The extent of the leakage flow depends on the size and shape of clearance paths and the pressure difference across these paths.

Table 1 summarizes the different types of positive displacement machines, their applications, type of leakages, and parts which create the clearance paths and the simplified clearance structure.

In recent studies [10–12], the isentropic nozzle equations and chamber models were used by the researchers to carry out the preliminary estimations of leakages in positive displacement machines. Utri et al. [10, 11] studied the fluid leakages through rotor tip housing clearances and end plate clearances in screw machines using dimensionless numbers. Further to this, investigations were also carried out on the leakages and the fluid-structure interactions using CFD simulations [4, 13]. The mass flow rates were determined using CFD simulation and compared with the analytical and experimental results and the influence of dimensionless numbers on the flow coefficients studied. Liang and Wu [14] proposed a mathematical model based on perfect gas laws, standard thermodynamic process, oil injection effects, oil-gas heat transfer, and internal leakages. The authors also presented values of different clearance paths as well as other important twin-screw compressor parameters. A summary of experimental studies on twin screw compressors suggests that cutting-edge techniques such as LDV/PIV can be explored to better understand and visualize the thermo-fluid-solid relationship in the compressor [15].

An experimental setup was used for simulating leakage flow and calculating the leakage rate through the blowhole clearance in a twin-screw compressor using an iterative approach [16, 17]. The study carried out the experimental work with circular convergent nozzles (of equivalent area to the blowholes considered in the study), and the findings were compared with the analytical results. It was suggested that the technique be used to model and estimate leakages in other positive displacement machines.

Vodicka et al. [18] conducted a theoretical and experimental study of the effect of various leakages on the operating efficiency of a rotary vane expander. A novel experimental method for axial and radial clearance adjustment has been developed. A 1-D mathematical model was developed (with a prediction accuracy of within 5%) using experimental data ranging from 0 to +0.5 mm clearance. Additionally, the model was used to optimize and evaluate the effect of reduced manufacturing tolerances on expander parameters. Lee et al. [19] used previously developed four mathematical models to measure leakage flow rates. The first model was based on isentropic nozzle equations and frictionless compressible flow. The second model was the Fanno flow model, which took adiabatic flow with fluid friction into account. Ishii's incompressible and viscous flow model was the third model, and the fourth was a 1D steady-state laminar flow model with friction between two parallel plates [20]. When the results from all four models were compared to the experimental results, it was discovered that the nozzle equation results were very similar to the experimental results. For various pressure ratios, the relationship between leakages and clearances is presented. Lee [21] proposed a simulation model for output prediction that takes into account both the compression process and the

dynamics of the moving parts. The compression process was modelled using the assumption of a working chamber as the control volume, to which the principles of mass and energy conservation were applied. To estimate the axial clearance leakages in the scroll compressor, Wang and Liu [22] proposed an updated Fanno flow model and turbulence model. The model results were compared to the experimental results, and the effects of pressure difference, clearance number, and spindle speed were investigated. The Fanno model was found to be more suitable for predicting leakages at lower rotational speeds and smaller clearances, while the turbulence model was found to be more suitable at higher rotational speeds and larger clearance sizes.

Pend et al. [23] developed a thermodynamic model of an oil-free scroll compressor using the gas state equation, conservation of energy, and the law of conservation of mass, as well as a heat transfer and leakage model. The leakage flow for each compression chamber was calculated using a thermodynamic model that used the improved Euler process. Imamoglu and Ertunc [24] presented a comparison of theoretical and numerical results of the tip leakages. The leakage geometry was simplified and numerical simulations were performed for four pressure differences and seven rotational speeds. The authors also presented an effect of heat transfer from the heated casing to the tip clearance fluid. Muhammad [25] unwrapped a twin-screw pump circumferential clearance and approximated it as a rectangular clearance and the same approach can be applied for other positive displacement machine clearances also.

Zhang et al. [26, 27] presented a 3D transient CFD numerical simulation model for a scroll compressor with dynamic meshing along with radial and axial clearance considerations. Radial leakage though had a greater effect on the volumetric performance than tangential leakage (specifically in hydrogen scroll pumps). Sun et al. [7, 28] performed a PIV test to obtain the velocity field around the tip gap and used SCORG™ (Screw Compressor Rotor Grid Generation) software to predict the leakage flow under same operating conditions. In the majority of areas, the main flow pattern and velocity magnitude were found to be the same in the CFD simulation as well as the experimental analysis, though the CFD study overestimated the leakage flow velocities. The CFD findings indicate the presence of a vortex produced by the leakage flow in the gap's downstream area. Flow losses in the tip gap occur mostly near the entry upstream of the gap. Ziviani et al. [29, 30] presented a leakage model describing nine leakage paths in a single screw expander. The model results found a good agreement within ±10% and ±15% for the mass flow rate and power, respectively. The authors also applied different grid generation approaches (both in the steady-state and transient conditions) and commercial software to identify the best suitable approach. For the steady-state simulation, a maximum deviation of 10% in results was observed between various simulations tools used, while for the transient simulation, only CS (Chimera strategy) simulation approach gave satisfactory results.

Kauder and Sachs [31] used Toepler's "Schlieren-method" to visualize the leakage flow in the male rotor housing gap of a screw-type machine. Additionally, the authors used a vortex flow meter to determine the mass flow rate through gaps of 0.1 mm, 0.2 mm, and 0.4 mm at a pressure ratio (downstream to upstream pressure as shown in Figure 1) of about 0.5. For pressure ratios, less than 0.5, the mass flow rates were determined using mass flow meters based on temperature differences at a heating element.

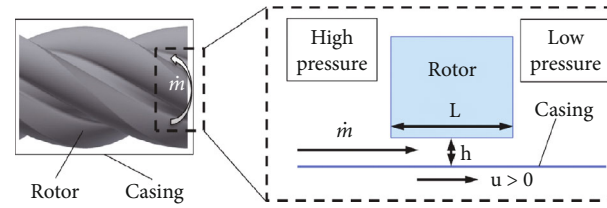

Figure 1: End plate clearance and the leakage flow from high-pressure chamber to low-pressure chamber [11].

In order to estimate the leakage flow in positive displacement machines, apart from the various experimental and numerical studies, various analytical models have been used by researchers. Kotlov et al. [5, 6] used a mathematical model to estimate the gas leakages from high-pressure cavities to low-pressure cavities in vane compressors and dry claw compressors. Kotlov et al. used the following equation to determine the leakage flow rate across the gap at different rotor positions:

$$\dot{m} = \Phi * A * \sqrt{\frac{\rho_2 * p_2 * (\varepsilon^2 - 1)}{\ln \varepsilon^2 + \xi + (\lambda * \sum)}}. \tag{1}$$

Utri et al. [10, 11] investigated flows through male rotor housing clearance and end clearance. The flow coefficients were determined using CFD simulation results and compared with analytical and experimental results available in the literature [32]. The study varied dimensionless quantities such as Reynolds number, specific heat ratio, Mach number, height to diameter ratio (in rotor tip housing leakage), height to length ratio (in end plate leakages), and pressure ratio to observe the individual influence of these dimensionless quantities on the flow coefficient. The study recommended two different simulation methods more suitable to predict the operational behavior in positive displacement machines, namely the CFD and the chamber model. The chamber model is more suitable when many configurations need to be simulated in comparison to the CFD model, which needs time-consuming computations. The chamber model considers the time-dependent geometric values of the chamber volumes, clearances, and port areas.

The mass and energy exchange between the chambers (shown in Figure 1) under consideration can be estimated using the following isentropic nozzle equations [33].

$$\dot{m}_{\text{ana}} = \frac{A p_1}{\sqrt{T_1}} \sqrt{\frac{2 * k * \left((r)^{2/k} - (r)^{k+1/k}\right)}{R\,(k-1)}} \quad \text{for } r > \left(\frac{2}{k+1}\right)^{\frac{k}{k-1}}, \tag{2}$$

Table 2: Geometry details of circular clearances (nozzles).

Nozzle number	Nozzle clearance—d (mm)	Upstream diameter of the nozzle—D (mm)	Nozzle area (mm^2)	β ratio
1	1.82	6.00	2.6	0.31
2	2.09	6.00	3.4	0.35
3	2.53	6.00	5.0	0.43
4	2.98	15.5	7.0	0.19
5	3.60	15.5	10.2	0.23
6	3.84	15.5	11.6	0.25
7	3.99	15.5	12.5	0.26

$$\dot{m}_{\text{ana}} = \frac{Ap_1}{\sqrt{T_1}}\sqrt{\frac{2*k}{R(k-1)}} * \left(\frac{2}{k+1}\right)^{\frac{k}{k-1}} \text{for } r < \left(\frac{2}{k+1}\right)^{\frac{k}{k-1}}. \tag{3}$$

The flow coefficient (Φ) can be defined as a ratio of the experimental leakage flow to the analytical leakage flow rate,

$$\Phi = \frac{\dot{m}_{\text{exp}}}{\dot{m}_{\text{ana}}}. \tag{4}$$

Utri et al. [10, 11] derived the theoretical mass flow rates by CFD-simulation using ANSYS CFX and compared the same with the experimental data from the work of Kauder and Sachs [31] to estimate the flow coefficient (Φ).

The estimation of leakage mass flows through gaps using isentropic nozzle equations and flow coefficients (to account for actual flow conditions) is the simplest and the most widely used analytical approach. However, the flow coefficients applied generally do not take into account the shape of these leakage paths. For that reason, a proper understanding of the relationship of flow coefficients and flow and shape parameters is critical for the accurate prediction of leakage flows. The present study investigates the influence of dimensionless numbers such as the Reynolds numbers, β ratios, Mach numbers, and pressure ratio on the flow coefficients for circular and rectangular clearance shapes. The flow coefficients were determined by comparing the experimental values obtained in an experimental test rig with the flow rates obtained from the simplified nozzle equation. The results obtained can be used for the evaluation of flow coefficients for other similar geometries, independent of the operating conditions. A quantitative approach is employed to estimate the leakage mass flow rate through the gaps (circular and rectangular) by using an experimental test rig involving testing of different size convergent nozzles (with circular gaps) and plates (with rectangular gaps) at various pressure ratio conditions. Eqn. (2) and Eqn. (3) are used to calculate the theoretical leakage flow rates and compared with the experimental leakages to determine the flow coefficients (using Eqn. (4)). The flow coefficients derived using experimental study are presented as a function of dimensionless numbers such as pressure ratio, Reynolds number, and Mach number.

Table 3: Geometry details of rectangular clearances (plates).

Plate number	Clearance width—w (mm)	Clearance height—h (mm)	Clearance areas (mm^2)	AR ratio
P1	40	0.180	7.2	0.0044
P2	45	0.200	9.0	0.0045
P3	44	0.250	11.0	0.0058
P4	80	0.250	20.0	0.0031

2. Experimentation Details

In a positive displacement machine, leakages occur through clearance paths of different sizes and shapes created by two or more stationary/moving components, as well as the pressure differential across these clearance paths. An experimental investigation was carried out to determine the leakages through various clearances of different sizes and shapes (at different pressure differences) to estimate the leakage rates and validate the analytical results. In the present work, the upstream pressure (P_1) is maintained constant, while the downstream pressure (P_2) varies to obtain different pressure ratios.

In the present study, the leakage mass flow rates were measured from seven nozzles (having circular clearances) and four plates (having rectangular clearances) at various pressure ratio conditions. Table 2 shows the geometry details of circular clearances of all the nozzles, while Table 3 shows the geometry details of rectangular clearances of all the plates.

2.1. Test Rig for Circular Clearance Leakages. The schematic of the test setup for simulating and determining leakages experimentally is shown in Figure 2 (for circular clearances) and Figure 3 (for rectangular clearances). A 22 kW constant speed twin-screw compressor was used to generate compressed air at 7.00 bar pressure, while the compressed airflow rate in the discharge line after globe valve (in both with and without leakage conditions) was measured with the help of CAV (Critical Arc Venturi) nozzle (Figure 4) as per ISO 1217 [34]. A 272-liter air receiver was used in the by-pass leakage line after the nozzle in order to collect the leaked air coming through the nozzle. To regulate the pressure inside the air-receiver and thereby maintain the pressure differential across the nozzle, one globe valve (Figure 4) installed in the discharge line and one ball valve (installed after the air-receiver tank) were used. The compressor discharge pressure, compressor discharge temperature,

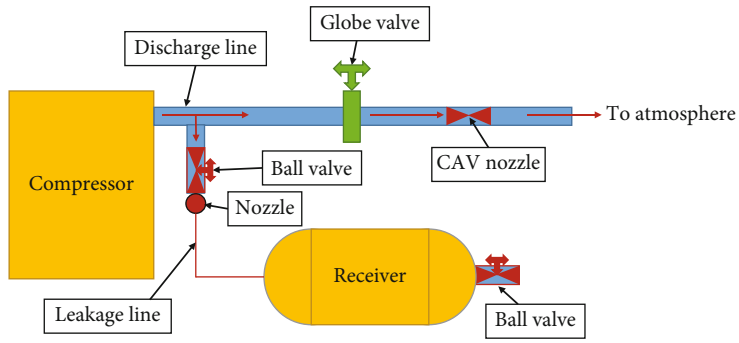

Figure 2: A schematic of the experimental setup (for circular clearance leakages).

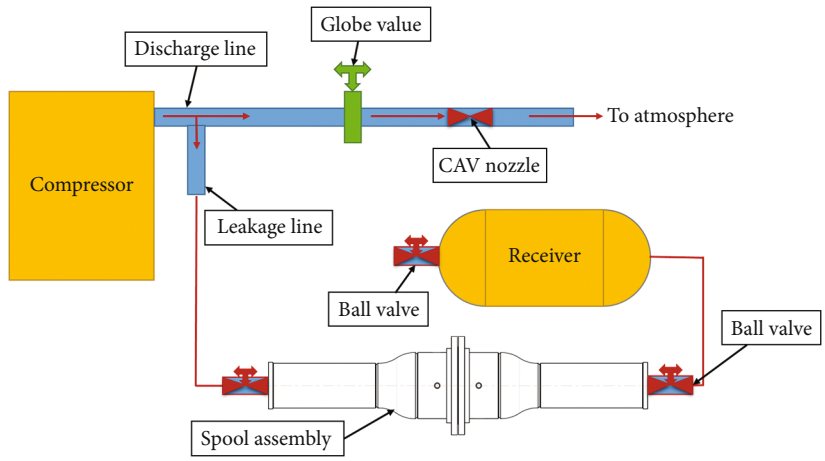

Figure 3: A schematic of the experimental setup (for rectangular clearance leakage).

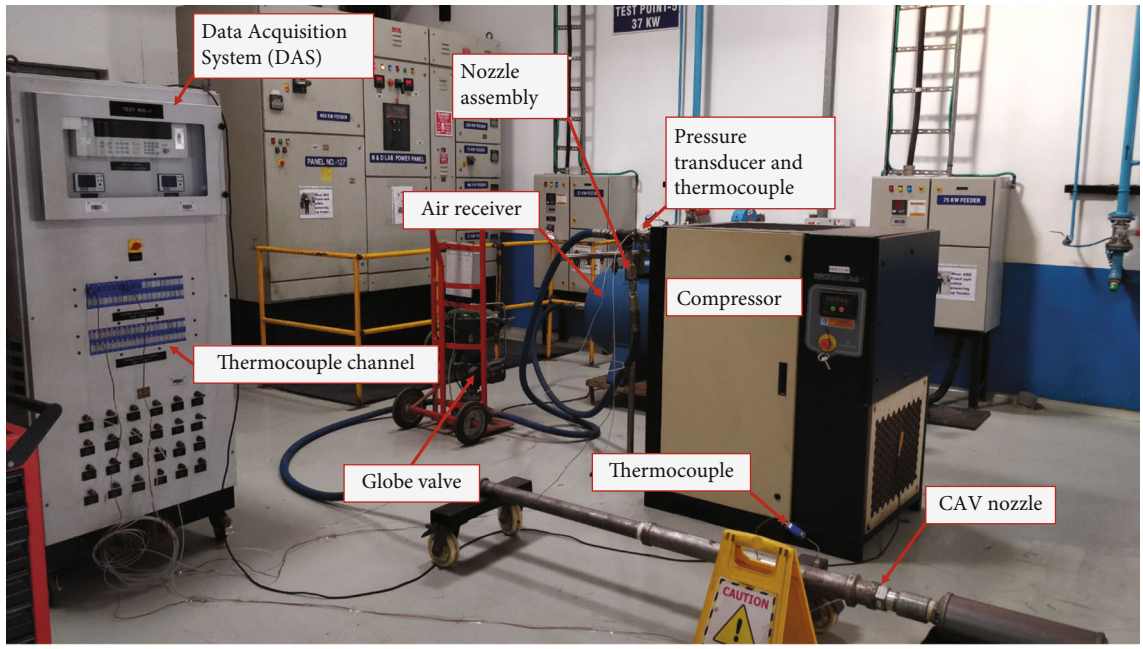

Figure 4: Photograph of experimental test rig (for circular clearance leakages).

CAV nozzle pressure and temperature, barometric pressure, and air-receiver pressure were recorded using various sensors connected to the DAS (Data Acquisition System) as shown in Figure 4. A ball valve after the tee connection was installed to isolate/connect the bypass leakage line with the mainstream. The convergent nozzles were installed in the leakage line (before the air receiver) to simulate leakages through seven different circular clearances at different pressure ratios. Table 2 summarizes the geometric details of the seven different convergent nozzles used in the experimental work, and Figure 5 shows the photograph and cross-section details of these nozzles.

2.2. Test Rig for Rectangular Clearance Leakages. Figure 3 shows a schematic of the test setup used to simulate the leakages through rectangular clearances. The setup is similar to the setup explained for the circular clearance leakages (in Section 3.2). The difference between this setup and the previous one (explained in Section 3.2) is the use of a spool assembly (with sandwiched plate) instead of a circular nozzle. The pressure differential across the plate (high-pressure and low-pressure chambers) and the clearances on the plates cause leakages. Figure 6 shows the photo of an actual spool assembly and a plate used in the experiments.

2.3. Test Methodology to Measure the Leakages. The present study involves simulation of the leakages occurring within the positive displacement machines with the help of an experimental test setup.

The test methodology (Figures 2 and 3) for the leakage measurement involved convergent nozzles/plates with the clearances and a specific pressure difference across the nozzle or the plate. A flow measurement (with and without the leakage line open) with a CAV nozzle provides an estimate of the leakage mass flow rate across the convergent nozzle or across the plate for a given pressure difference. Initially, the complete flow without any leakage was considered in the experiment by closing the leakage line (Case 1), in which all of the pressurized air from the compressor flowed through the CAV nozzle at a pressure of 7 bar. After opening the leakage line (Case 2), the flow was allowed to leak through the circular/rectangular clearance at a predetermined pressure difference. The difference in flow calculated between Case 2 and Case 1 (using a CAV nozzle) is perceived as an experimental calculation of leakage for the specific clearance and pressure difference combination.

The following are the details of the testing for both cases:

Case 1. Flow measurement considering no leakage.

In this case, of zero leakage, the leakage line was isolated from the discharge line by closing the ball valve installed before the convergent nozzle. The compressed airflow at 7.00 bar was measured in the discharge line as per ISO 1217 with the help of a CAV nozzle.

Case 2. Flow measurement considering leakages.

In this case, the compressed air leakage was allowed to leak through the clearances on the convergent nozzle/plate installed in the leakage line by keeping the ball valve fully open. The globe valves (installed on the air-receiver and installed in the discharge line) and the discharge ball valve (installed before the CAV nozzle) were used to maintain the desired pressure difference across the convergent nozzle/plate.

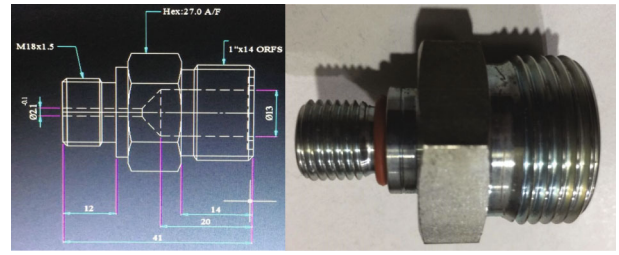

Figure 5: The convergent nozzle photograph and details.

The following are the parameters captured for each set of reading using sensors and data acquisition system (shown in Figures 4 and 6), to calculate the mass flow rate.

(i) Ambient temperature

(ii) Package discharge temperature

(iii) Nozzle temperature

(iv) Relative humidity

(v) Package out pressure

(vi) Before clearance pressure

(vii) After clearance pressure

(viii) Barometric pressure

(ix) CAV nozzle pressure

2.4. Uncertainty Analysis. The details of the equipment/instruments used in the experimentation along with the uncertainty involved are shown in Table 4.

The total airflow uncertainty at the confidence level of 95% is calculated as per the following equation:

$$U_{95} = \sqrt{B_w{}^2 + (t_{95}\, S_w)^2}, \tag{5}$$

wherein the flow measurement standard deviation (B_w) and systematic error (S_w) can be derived using the following equations:

$$B_w = \dot{m}\sqrt{\left(\frac{B_{P1}}{P_1}\right)^2 + \left(\frac{-B_{T1}}{2T_1}\right)^2 + \left(\frac{B_C}{C}\right)^2 + \left(\frac{2B_d}{d}\right)^2},$$
$$S_w = \dot{m}\sqrt{\left(\frac{S_{P1}}{P_1}\right)^2 + \left(\frac{-S_{T1}}{2T_1}\right)^2 + \left(\frac{S_C}{C}\right)^2 + \left(\frac{2S_d}{d}\right)^2}. \tag{6}$$

The method defined in ISO 5168:2005 [35] was used to estimate the uncertainty in the experiment. With a confidence level of 95%, the total airflow ($\dot{m}$) uncertainty was found to be 1.29% based on the measured parameters.

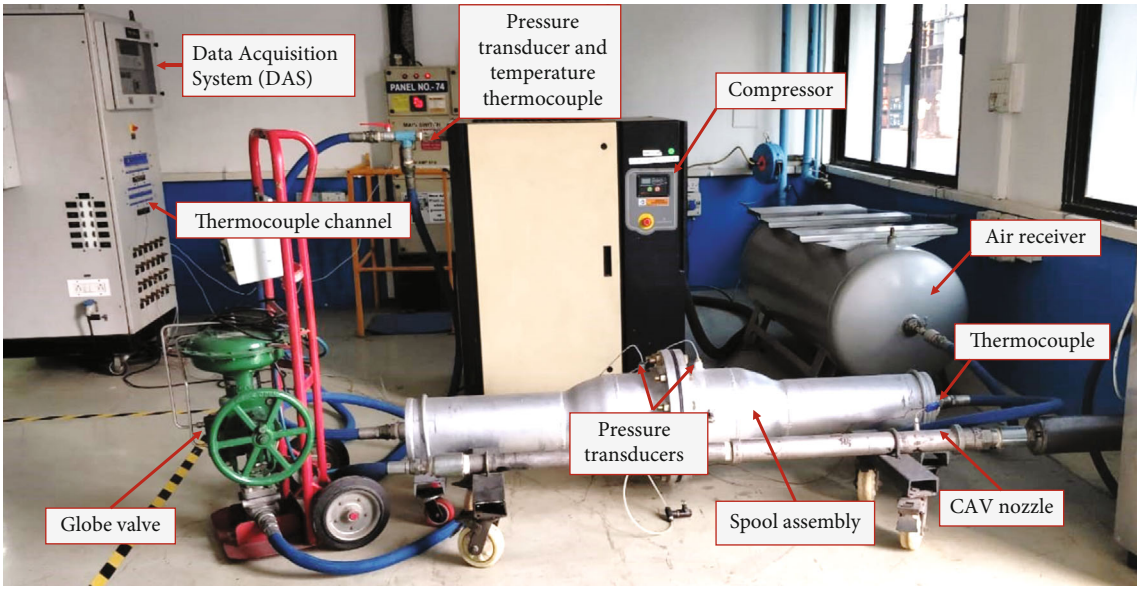

Figure 6: Photograph of experimental test rig (for rectangular clearance leakages).

Table 4: The details of the equipment/instruments used in experimentation.

Equipment/instrument	Model	Make	Uncertainty	Specification
Twin-screw compressor	RS22-7-AC	Ingersoll Rand	—	Oil flooded twin-screw compressor 22 kW, 7 bar, 140 CFM
Air receiver—horizontal	272 liter	Ingersoll Rand	—	272-liter air receiver
Data acquisition system (DAS)	34980A	Agilent	—	140 channel universal input and connectivity to lap top for real time monitoring and capturing the readings
Pressure transducer	245 series	Viatran	±0.1%	Measuring range—0 to 300 psig
T type thermocouple	TQSS-18 U-6	Omega	0.5^0 C	Measuring range—200 to 350°C
Barometric pressure gauge	CPG2400	Mensor	0.03%	Measuring range—8-17 psia
CAV pressure gauge	CPG2400	Mensor	0.03%	Measuring range—0-100 psig
Globe valve with actuator	GX + FIELDVUE DVC6200	Emerson	±0.5%	Minimum recommended supplied pressure: 0.3 bar (5 psig) higher than maximum actuator requirements Maximum: 10.0 bar (145 psig) or maximum pressure rating of the actuator, whichever is lower Medium: Air or natural gas Independent linearity Typical value: ±0.50% of output span

3. Results and Discussions

The experimental results from the study are compared with the analytical results to calculate the flow coefficients and presented in the form of dimensionless numbers such as the Reynolds number, the Mach number, and the pressure ratio. The flow coefficients are evaluated for circular and rectangular clearances at various pressure ratios based on the experimental and analytical study.

3.1. Experimental and Analytical Results: Circular Clearances. The analytically (using isentropic nozzle equations) and experimentally determined leakage mass flow rates through the circular clearances (for $D = 6.0$ mm and $D = 15.5$ mm) are compared and presented in Figure 7. The leakage rates are obviously higher for larger clearance areas and lower pressure ratios (higher pressure difference). In comparison to the experimental leakage mass flow rates, the analytical approach (using Eqn. (2) and Eqn. (3)) overestimates the leakage mass flow rates. The analytical method's overprediction (for all clearances and pressure ratios) is due to the assumption of frictionless flow consideration which differs from the actual conditions and existence of friction in practice. The results also indicate that, because of the choked flow situation, the leakage rates below pressure ratio 0.528 (critical pressure ratio) remain nearly constant. The similar trends of choked flow

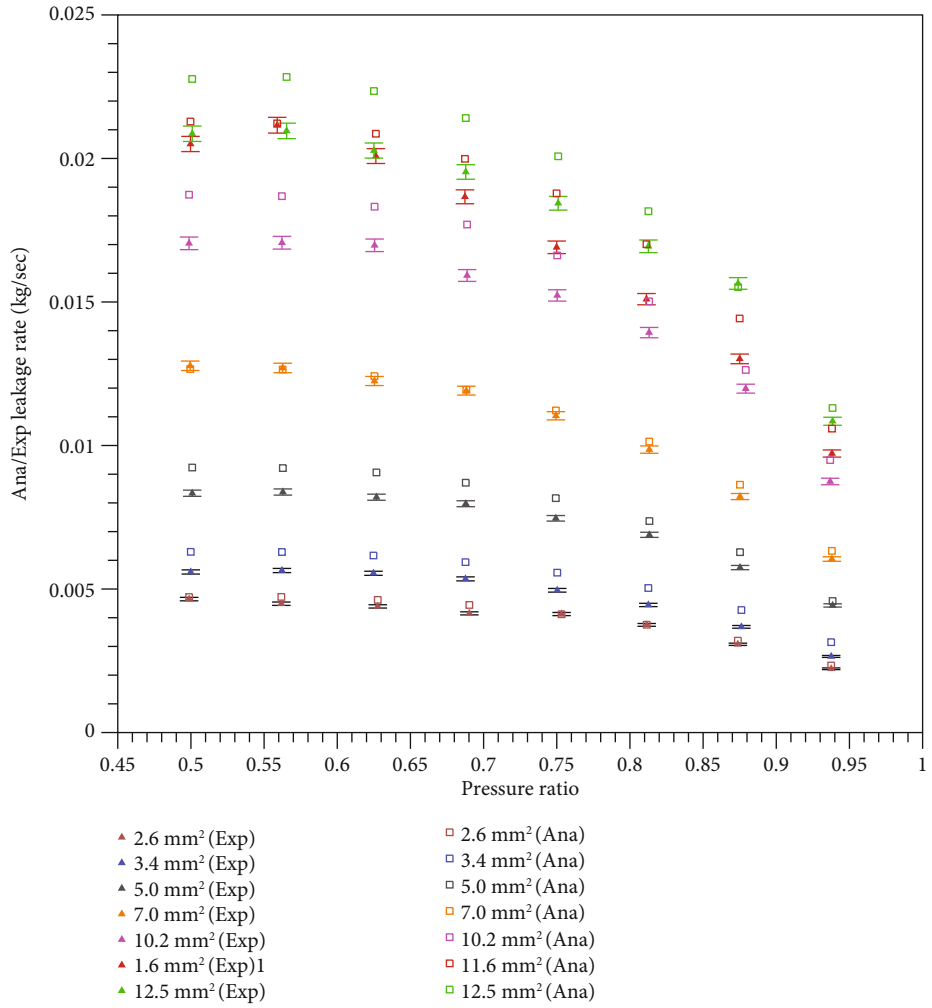

Figure 7: Experimentally and analytically determined leakage mass flow rate (kg/sec) as a function of pressure ratio for circular clearances (nozzles with $D = 6.00$ mm and $D = 15.50$ mm).

condition below the critical pressure ratio (PR < 0.528) have been reported by Utri et al. [10, 11]. This implies that, after this point, the decrease of the downstream pressure has no influence on the leakage flow through the clearance.

For all clearance sizes, Figure 8 shows the flow coefficient as a function of pressure ratios. Two distinct plots are provided to compare the flow coefficients at $D = 6.00$ mm and $D = 15.5$ mm, since the trend of the change in flow coefficient was found to be different in both cases. In the case of nozzles with an upstream diameter of $D = 6.00$ mm, the flow coefficients are found to increase with decreasing pressure ratios, indicating that isentropic nozzle equations are justified for lower pressure ratios. This is due to higher velocity and lower local resistance when the pressure ratio is low. The temperature and dynamic viscosity does not change; however, kinematic viscosity decreases for a higher value of downstream pressure. In the case of an upstream diameter of $D = 15.5$ mm, the flow coefficients for all pressure ratios justify the isentropic nozzle calculations since the flow coefficients are higher (above 0.89, almost constant or slightly increasing) over the entire pressure ratio range. This is due to the greater converging area of the nozzle in comparison to the nozzle with an upstream diameter of $D = 6.00$ mm and a lower local resistance. The flow coefficients for the entire pressure ratio spectrum (all clearance areas) are in the range of 0.85 to 0.96, which is reasonably high and justify the isentropic nozzle equation consideration.

For $D = 6.00$ mm, Figure 9(a) shows that the flow coefficients increase as the Reynolds number increases, which is due to the increased velocity and decreased friction. The isentropic nozzle equation assumptions are well supported by this low friction conditions. In Figure 9(b), the flow coefficients for $D = 15.5$ mm remained nearly constant (marginally decreasing) as the Reynolds number increases, which can be attributed because of the combined effects of the geometry (in comparison to $D = 6.00$ mm nozzles) and the uncertainty of the experimental results.

The flow coefficient is plotted as a function of the Reynolds number for various Mach numbers in Figure 10. For nozzles with an upstream diameter of $D = 6.00$ mm (Figure 10(a)), the flow coefficients decrease as the Reynolds number increases, which is not normal and is due to the geometry

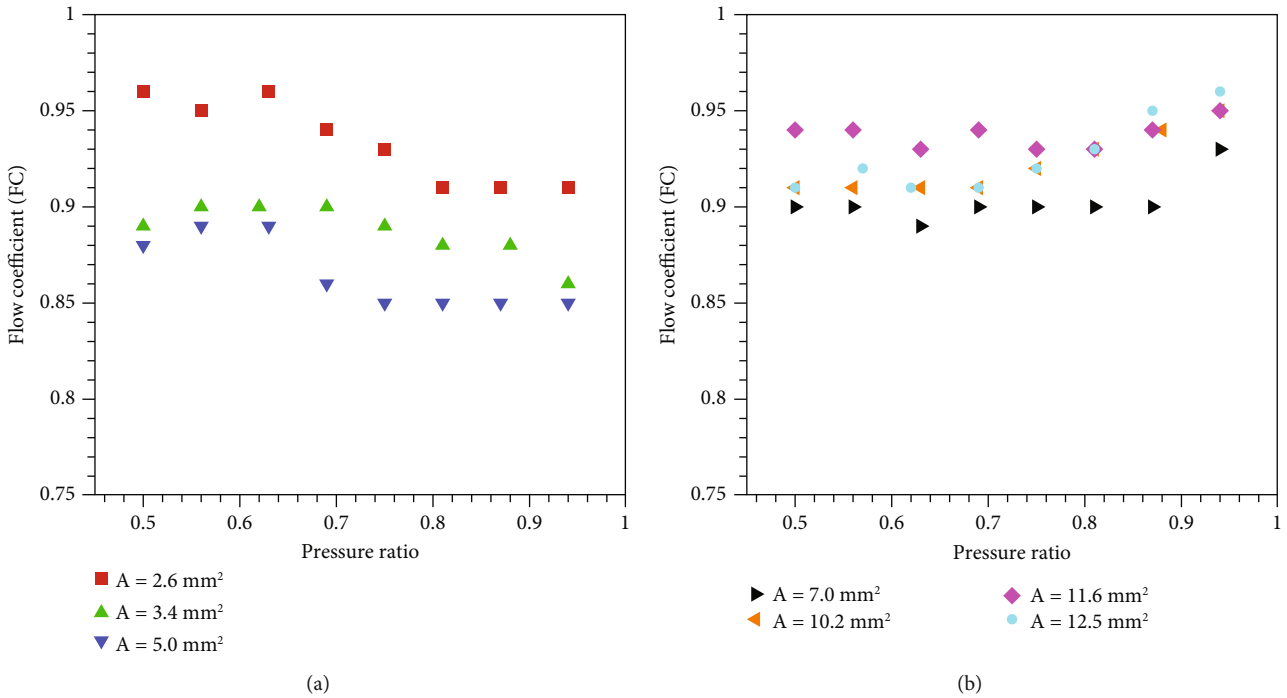

Figure 8: Flow coefficient (FC) as a function of pressure ratio for all the circular clearances (nozzles with $D = 6.00$ mm and $D = 15.5$ mm).

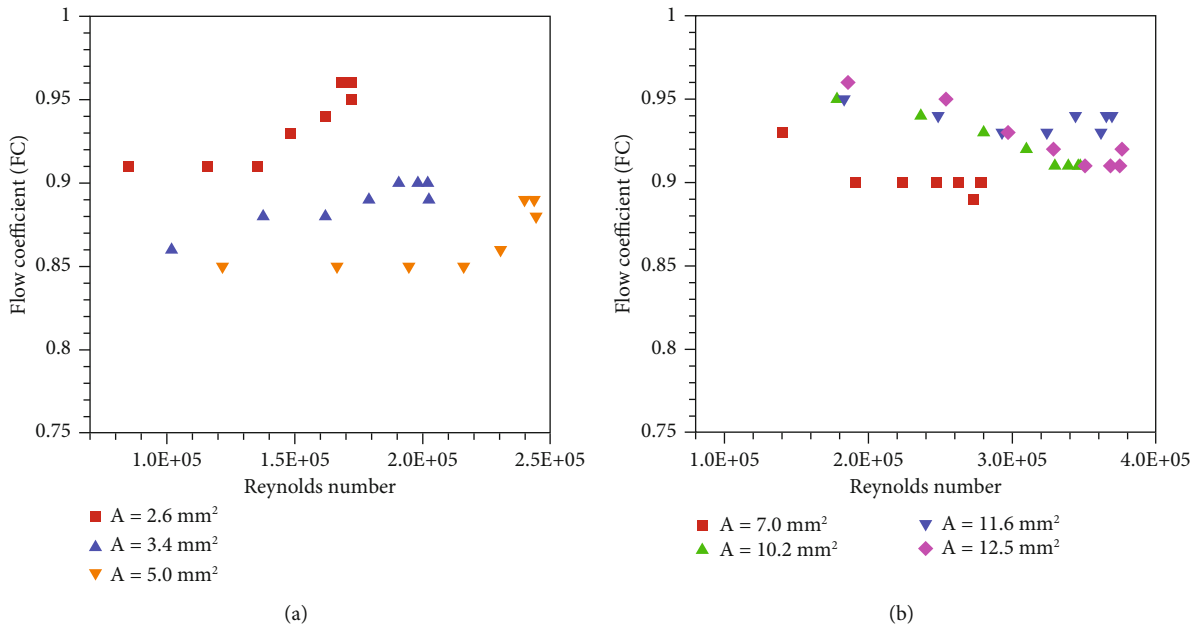

Figure 9: Flow coefficient (FC) as a function of Reynolds number for different leakage clearances.

and experimental uncertainty. The flow coefficient increases as the Mach number increases (velocity increase and friction decreases), indicating that flow velocity has a significant effect on the experimental leakage rate. In the case of nozzles with an upstream diameter $D = 15.5$ mm (Figure 10(b)), the behavior is opposite. Because of the lower value of friction, the flow coefficient increases with increasing Reynolds number, which justifies the isentropic nozzle equations.

Reynolds number (Re) depends on hydraulic diameter, velocity, density, and viscosity. In this study, the temperature is almost constant (and that is why dynamic and kinematic viscosity does not have significant change and effect on the Reynolds number) and that is why Reynolds number (Re) mainly depends on hydraulic diameter and velocity. However, in the case of higher Mach numbers (for Ma >0.686), there is a little effect on the flow coefficient for all Reynolds

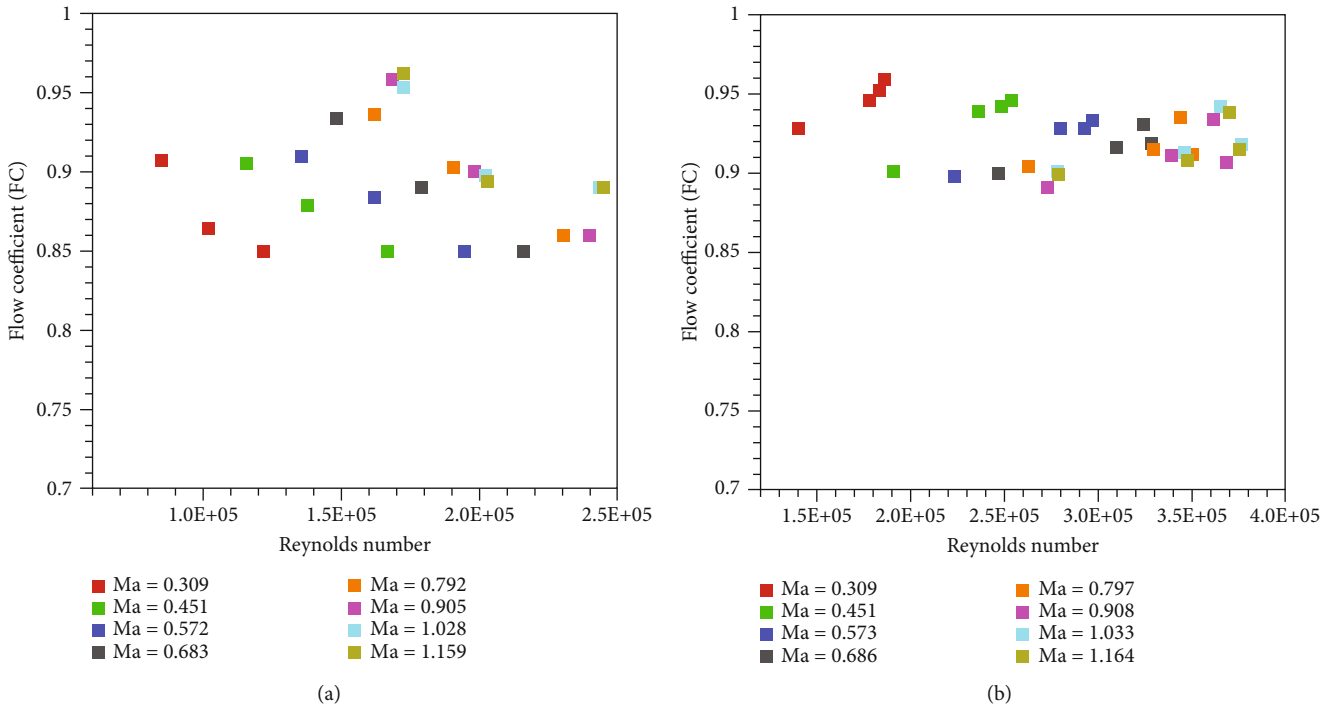

Figure 10: Flow coefficient (FC) as a function of Reynolds number for different Mach number.

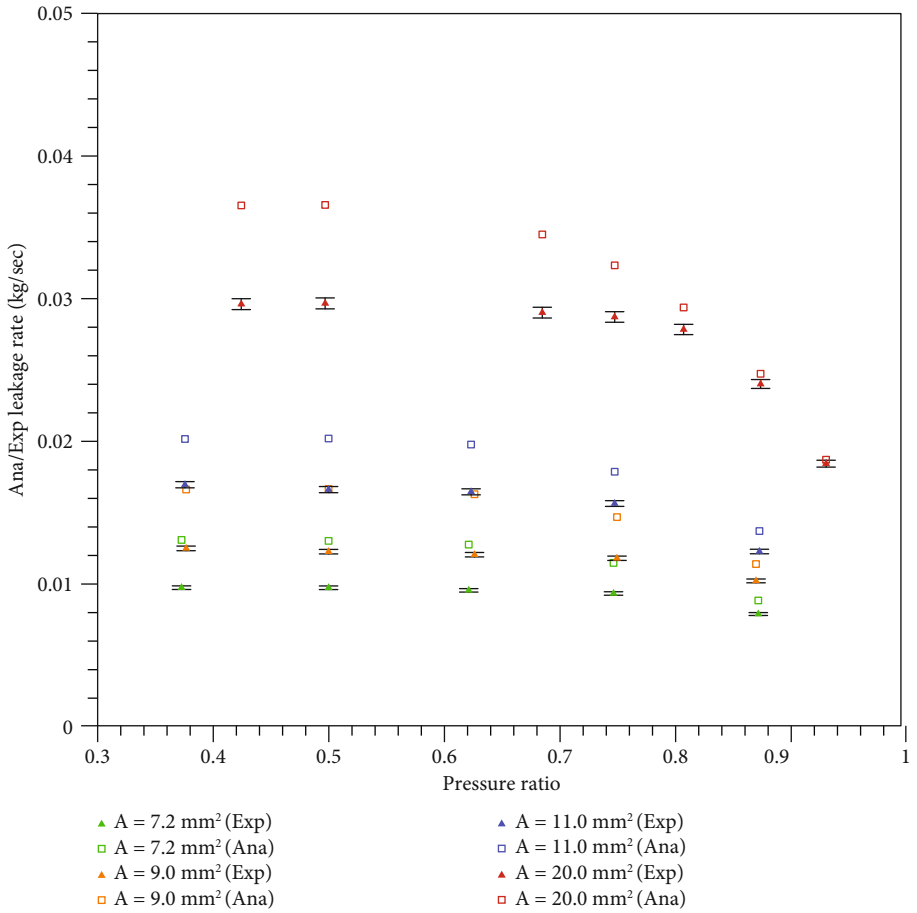

Figure 11: Experimentally and analytically determined leakage mass flow rates (kg/sec) as a function of pressure ratio for different clearance areas (all plates).

numbers, indicating that velocity has no effect on the actual flow and flow coefficient above a certain value.

3.2. Experimental and Analytical Results: Rectangular Clearances. The circular plates with different size rectangular slits were used in the experimental setup (Figure 6) to simulate the leakages through the rectangular clearances at different pressure ratios. The analytical and experimental leakage flow rates across rectangular clearances (with varying clearance sizes) in terms of pressure ratio are depicted in Figure 11. The findings demonstrate that the analytical method, which assumes frictionless flow, overestimates the leakage flow in relation to the real flow. Similar to circular clearances, the choked condition is observed below the critical pressure ratio. For the same clearance size, the leakage rate increases with increasing pressure difference (decrease in pressure ratios). The leakage rate increases as the clearance height increases (for plates P1, P2, and P3, which have nearly identical widths) for the same pressure ratio. The leakage rate of plate P4 is nearly twice that of plate P3, which is because of double the width of clearance (compared to the width of plate P3) for the same clearance height. This indicates that, in addition to the pressure ratio, the clearance height and clearance distance have an impact on leakages.

Figure 12 shows the flow coefficient as a function of pressure ratio for all clearance areas. In contrast to circular clearance, the flow coefficient improves as the pressure ratio rises. This indicates that at lower pressure ratios, the rectangular clearance provides more resistance (and therefore more friction) than the circular clearance. For all plates below the critical pressure ratio, the flow coefficients are unchanged, indicating a choked condition for both the analytical and experimental results. The flow coefficient increases as the clearance height increases (for the same width), which is because of reduced friction and reduced local resistance. Additionally, the flow coefficients are almost identical for plates (plate P3 and P4) of equal clearance height but different clearance areas (plate P4 is having double clearance area than plate P3), indicating that clearance height has a greater effect on the flow coefficient than clearance width under the same pressure condition. This means that the influence of friction is the same on both the plate P3 and P4 of the same clearance height but different widths.

Figure 13(a), which plots the flow coefficient as a function of Reynolds number, suggests that the flow coefficient decreases as the Reynolds number increases, which is not typical and is due to the geometry's local resistance and experimental uncertainty. Increases in clearance size increase the flow coefficient for the same Reynold number resulting in lower friction in larger leakage areas. It is observed that for a given Reynold number, the flow coefficients are identical for different clearance areas but the same clearance height, indicating that the clearance height plays a significant role in offering friction. The flow coefficient is plotted as a function of Reynolds number for various Mach numbers in Figure 13(b). This shows that the flow coefficient increases as the Reynolds number increases for a given Mach number. Additionally, the plot demonstrates that decreasing the Mach number increases the flow coefficient at a given Reynolds number, which is due to the reduced velocity. The flow coefficients do not change significantly with increasing Mach number (above Ma = 0.91) for the same Reynold number, indicating that the velocity above one limit has no major impact on the leakage rate.

Analytical findings are obtained for both circular and rectangular clearances using the nozzle equations, which assume frictionless flow and leakage clearance area rather than leakage clearance geometry. When leakages are determined experimentally, they take clearance size, clearance shape, friction, and local resistance into account. That is why flow coefficients are proportional to dimensionless numbers, such as the Reynolds number, the Mach number, the aspect ratio, and the beta ratio. In comparison to circular clearances, rectangular clearances have a wider range of flow coefficients between 0.74 and 0.98 due to the more influence of dimensionless numbers on the flow and flow coefficient. This implies that the convergent nozzle equation for analytical calculations in rectangular clearances requires suitable modifications and reconsiderations.

In this analysis, circular and rectangular clearances are used to simulate and estimate the real leakage through the positive displacement machines' clearances. However, in actual systems, numerous geometric parameters (including actual shapes, curves/profiles of key components, and dynamics of parts that generate clearances) and operational parameters (temperature, speed, gas property, and so on) affect leakage flows and flow coefficients, necessitating further study. Furthermore, the form of system and application (pumping, extension, compression, and flow control) have an effect on the leakage flow. The current study's methods and technique can be applied to several positive displacement devices with different applications, geometries, and operating conditions and the findings can differ accordingly.

3.3. Development of Empirical Correlation. The flow coefficient (Φ) is a function of nondimensional numbers such as the Reynolds number (Re), Mach number (Ma), pressure ratio (PR), and beta ratio (β) or aspect ratio (AR). The flow coefficient (Φ) functional relationship can be written as

$$\begin{aligned}&\text{Flow coefficient for the rectangular clearance } \Phi = fn\,(Ma, \text{Re}, PR, AR),\\ &\text{Flow coefficient for the circular clearance } \Phi = fn\,(\beta, \text{Re}, Ma, PR).\end{aligned} \tag{7}$$

The experimental results are used to develop these correlations of flow coefficient as a function of dimensionless numbers. In order to establish a relationship between flow coefficient (Φ) and Mach number (Ma) for the rectangular clearances, the values of ln (Φ) are plotted against ln (Ma) (not shown here) and a regression analysis to fit a second-order polynomial equation yielded:

$$\ln(\Phi) = m_1[\ln(\text{Ma})]^2 + m_2 \ln(\text{Ma}) + A_1, \tag{8}$$

where $m_1 = 0.0869$ and $m_2 = -0.1064$.

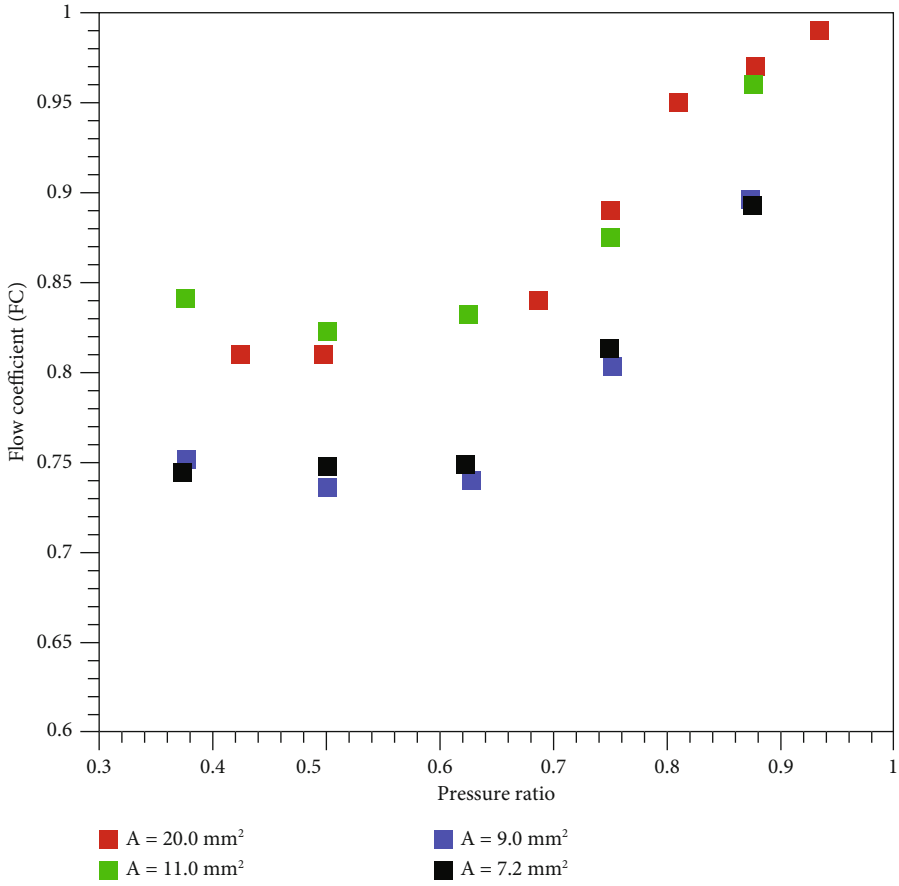

Figure 12: Flow coefficient (FC) as a function of pressure ratio for all plates.

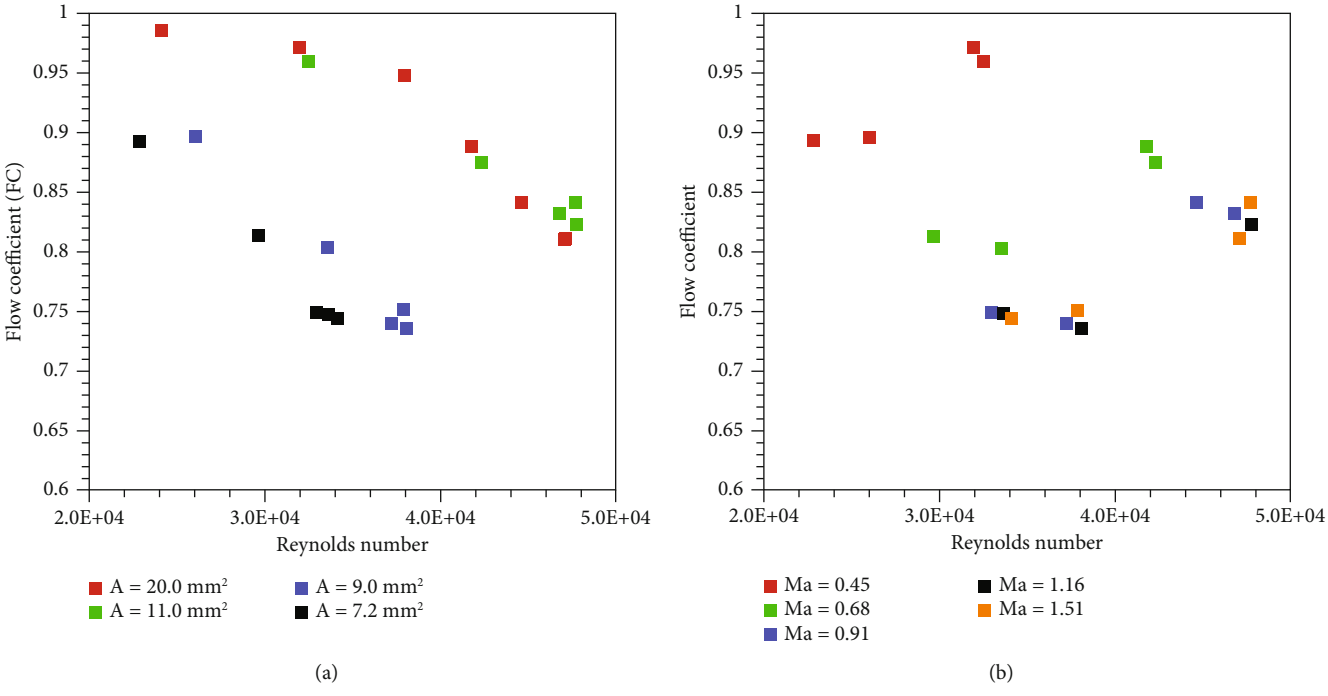

Figure 13: Flow coefficient (FC) as a function of Reynolds number for (a) different clearance areas and (b) different Mach Numbers.

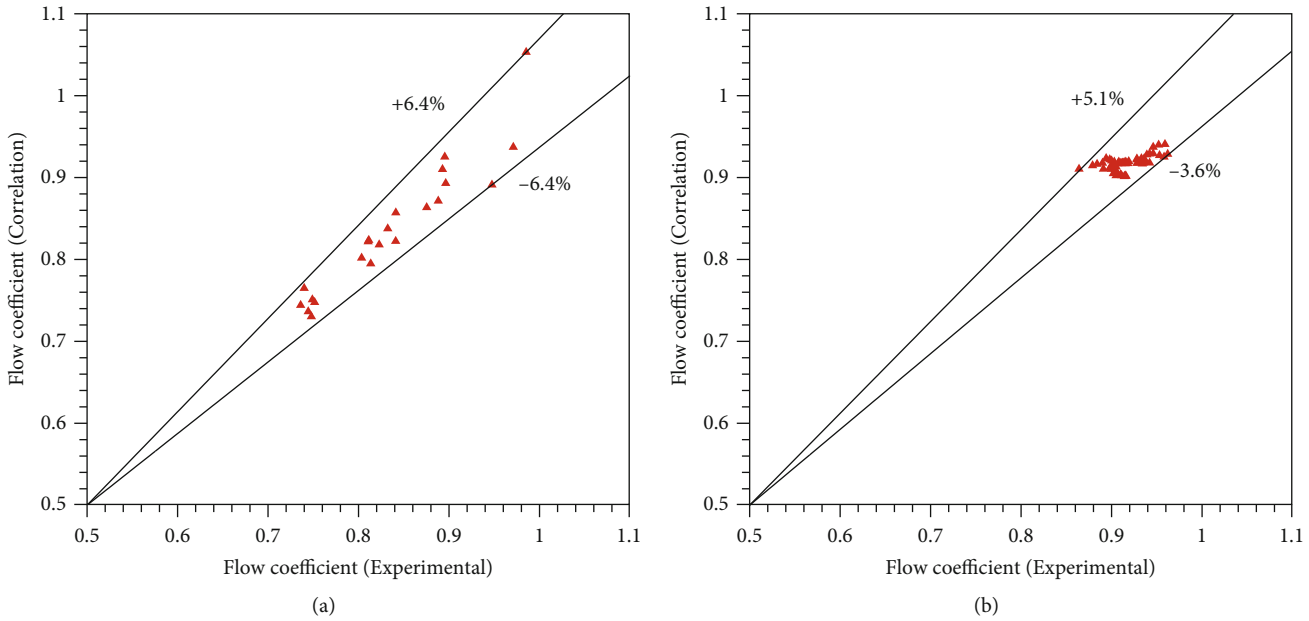

Figure 14: A comparison of predicted and experimental values of flow coefficients. (a) Rectangular clearance. (b) Circular clearance.

The functional relationship between Φ and Ma is rewritten as

$$\Phi = A_0 * (\mathrm{Ma})^{m_2} * \exp\left(m_1 (\ln (\mathrm{Ma})^2\right), \tag{9}$$

where A_0 is anti-ln of A_1

$$A_0 = \frac{\Phi}{(\mathrm{Ma})^{-0.1064} * \exp\left(0.0869\left(\ln (\mathrm{Ma})^2\right)\right.}. \tag{10}$$

In equation (10), A_0 is a function of Reynolds number (Re), the values of ln (A_0) are plotted against ln (Re) and a regression analysis to fit a second-order polynomial equation yielded:

$$\ln (A_0) = m_1 [\ln (\mathrm{Re})]^2 + m_2 \ln (\mathrm{Re}) + B_1, \tag{11}$$

where $m_1 = 0.3644$ and $m_2 = -7.4892$.

The functional relationship between A_0 and Re is rewritten as

$$A_0 = B_0 * (\mathrm{Re})^{m_2} * \exp\left(m_1 (\ln (\mathrm{Re})^2\right), \tag{12}$$

where B_0 is anti-ln of B_1.

$$B_0 = \frac{A_0}{(\mathrm{Re})^{-7.4892} * \exp\left(0.3644\left(\ln (\mathrm{Re})^2\right)\right.}. \tag{13}$$

From equations (10) and (13),

$$\Phi = B_0 * (\mathrm{Ma})^{-0.1064} * \exp\left(0.0869\left(\ln (\mathrm{Ma})^2\right)\right. * (\mathrm{Re})^{-7.4892} * \exp\left(0.3644\left(\ln (\mathrm{Re})^2\right)\right. . \tag{14}$$

A similar procedure is used to obtain the relationships between flow coefficient (Φ) and other parameters pressure ratio (PR) and aspect ratio (AR). The plots of ln (B_0) vs. ln (PR) and ln (C_0) vs. ln (AR) are plotted for second-order polynomial equations.

The final relationships (rectangular clearance) of flow coefficient obtained by these plots (not shown) are written below:

$$\begin{aligned}\Phi = 3.11e^{21} * (\mathrm{Ma})^{-0.1064} * \exp\left(0.0869\left(\ln (\mathrm{Ma})^2\right)\right. \\ * (\mathrm{Re})^{-7.4892} * \exp\left(0.3644\left(\ln (\mathrm{Re})^2\right)\right. \\ * (\mathrm{PR})^{-0.266} * \exp\left(0.2047\left(\ln (\mathrm{PR})^2\right)\right. \\ * (\mathrm{AR})^{4.1378} * \exp\left(0.381\left(\ln (\mathrm{AR})^2\right)\right. .\end{aligned} \tag{15}$$

A similar procedure is used to develop a correlation for flow coefficient (Φ) of circular clearance with regression analysis of data obtained from experimental investigations which gives

$$\begin{aligned}\Phi = 7.91e^{-4} * (\beta)^{-0.3892} * \exp\left(-0.1495\left(\ln (\beta)^2\right)\right. * (\mathrm{Re})^{1.11} \\ * \exp\left(-0.0452\left(\ln (\mathrm{Re})^2\right)\right. * (\mathrm{Ma})^{0.0194} \\ * \exp\left(0.0266\left(\ln (\mathrm{PR})^2\right)\right. * (\mathrm{PR})^{0.0157} \\ * \exp\left(-0.0212\left(\ln (\mathrm{PR})^2\right)\right. .\end{aligned} \tag{16}$$

Figure 14 shows a comparison between the experimental values of Φ and its predicted values by the correlation developed as per equations (15) and (16). The observation is made that the data lies between ±6.4% of the predicted values for the rectangular clearances and between -3.6% and +5.1 of the predicted values for the circular clearances.

4. Conclusions

Leakages through different clearance gaps are important in positive displacement machines, and an accurate prediction of the leakage flows needs an accurate knowledge of the flow coefficients, which are used along with nozzle equations to account for the actual prevailing flow conditions in machines. The present study examines the flow coefficients and investigates the influence of dimensionless numbers on the flow coefficients for circular and rectangular clearance shapes. The derived flow coefficients in terms of dimensionless numbers can be used along with the isentropic nozzle equations to estimate the leakages in any positive displacement machine.

The following are the key findings from the study:

(i) The flow coefficients vary from 0.88 to 0.96 for the circular clearance, which indicates that the consideration of convergent nozzle assumption is justified in circular clearances. In contrast to leakages through circular clearances, the experimental leakage flows through rectangular clearances are more affected by the Reynolds number, pressure ratios, Mach number, and beta ratio. As the theoretical leakage flows do not account for frictional effects, the impact of the dimensionless number on the experimental leakage flows results in a wide range of flow coefficients ranging from 0.74 to 0.98 for rectangular clearances

(ii) For all circular clearances, the flow coefficients are observed to be either increasing or remain nearly constant as the Reynolds number increases, which is due to increased velocity (and decrease in friction factor). In rectangular clearances, the flow coefficient decreases as the Reynolds number increases, which is not typical and could be due to the geometry's local resistance and experimental uncertainty. It is observed that for a given Reynolds number, the flow coefficients are identical for the same clearance height and different clearance width, indicating that the clearance height plays a significant role in offering friction

(iii) Below the choked flow conditions and critical pressure ratio ($r = 0.528$), the leakage flow remains constant and there is little difference between the analytical and experimental leakage rates (and constant flow coefficients) for the circular and rectangular clearances

(iv) It is observed that in the case of circular clearances, the mean deviation of the experimental leakage results (in comparison to the analytical results using isotropic nozzle equations) is +9.1%, which is significantly lower than the mean deviation (+20.5%) in the case of rectangular clearance leakages. The study indicates that the isentropic nozzle equation method is more suitable for predicting the leakages through the circular clearances and needs modifications for consideration of the rectangular clearances

(v) Using regression analysis, empirical correlations are developed to predict the flow coefficient in terms of Reynolds number, Mach number, pressure ratio, aspect ratio, and β ratio, which are found to match within ±6.4 percent of the numerical results for the rectangular clearance and within the range of -3.6 percent to +5.1 percent of the numerical result for the circular clearance

Nomenclature

$\dot{m}$: Leakage mass flow rate (kg/sec)
Φ: Flow coefficient (dimensionless)
A: Clearance leakage area (m^2)
ρ_2: Downstream density (kg/m3)
ε: Ratio of pressure P_1 (upstream) to P_2 (downstream)
ξ: Local resistance coefficient at a gap entry
λ: Friction factor
Σ: Form factor
T_1: The upstream temperature (K)
P_1: The upstream pressure (Pa)
P_2: The downstream pressure (Pa)
R: Gas constant of oil gas mixture (J/kg-K)
k: Specific heat ratio (dimensionless)
r: Ratio of pressure P_2 (downstream) to P_1 (upstream)
β: Diameter ratio (dimensionless)
AR: Aspect ratio (clearance height to width ratio) (dimensionless)
U_{95}: Total airflow uncertainty at confidence level of 95%
B_W: Systematic error in the flow measurement
S_W: Standard deviation in the flow measurement
S_{P1}: Experimental standard deviation for pressure (Pa)
S_{T1}: Experimental standard deviation for temperature (K)
S_C: Experimental standard deviation for discharge coefficient
S_d: Experimental standard deviation for throat diameter (m)
B_{P1}: Systematic error for pressure (Pa)
B_{T1}: Systematic error for temperature (K)
B_C: Systematic error for discharge coefficient
B_d: Systematic error for throat diameter (m)
d_t: Throat diameter (m)
D: Upstream diameter in nozzle (m)
d: Circular clearance diameter in nozzle (m)
w: Rectangular clearance width (m)
h: Rectangular clearance height (m)
Re: Reynolds number (dimensionless)
Ma: Mach number (dimensionless)
Exp/exp: Experimental
Ana/ana: Analytical
1: Upstream
2: Downstream.

Abbreviations

P-V: Pressure Volume
CFD: Computational Fluid Dynamics

ISO: International Organization for Standardization
CAV: Critical Arc Venturi
DAS: Data Acquisition System
FC: Flow Coefficient
LDV: Laser Doppler Velocimetry
PIV: Particle Imaging Velocimetry.

Data Availability

The data supporting the results of this study may be obtained from the corresponding authors as required.

Conflicts of Interest

The authors declare that there is no conflict of interest regarding the publication of this paper.

Acknowledgments

The authors acknowledge the support received from Ingersoll-Rand (India) Limited and Ingersoll-Rand USA for conducting the experimental work.

References

[1] World Energy Council, *World energy perspectives energy efficiency policies - a straight path towards energy sustainability*, 2016.

[2] V. M. Braga and C. J. Deschamps, "Numerical analysis of gas leakage in the piston-cylinder clearance of reciprocating compressors considering compressibility effects," in *IOP Conference Series: Materials Science and Engineering*, vol. 232, p. 9, United Kingdom, 2017.

[3] L. R. Silva and C. J. Deschamps, "Modelisation des fuites de gaz dans les soupapes du compresseur," *International Journal of Refrigeration*, vol. 53, pp. 195–205, 2015.

[4] R. Andres, J. Hesse, H. Babic et al., "CFD simulation of a twin screw expander including leakage flows," in *International Compressor Engineering Conference*, Germany, 2016.

[5] A. Kotlov, L. Kuznetsov, and B. Hrustalev, "Investigation of the influence of the number of vanes on the performance of a rotary vane compressor," *MATEC Web of Conferences*, vol. 245, p. 04008, 2018.

[6] A. A. Kotlov, I. A. Maksimenko, and Y. L. Kuznetsov, "The influence of profile geometric parameters on characteristics of rotor-gearing compressor," *IOP Conference Series: Materials Science and Engineering*, vol. 425, no. 1, p. 11, 2018.

[7] S. Sun, G. Singh, A. Kovacevic, and C. Bruecker, "Experimental and numerical investigation of tip leakage flows in a roots blower," *Designs*, vol. 4, no. 3, p. 17, 2020.

[8] C. Rong and W. Wen, "Compresseur a mesospirale : discussion sur les caracteristiques des fuites," *International Journal of Refrigeration*, vol. 32, no. 6, pp. 1433–1441, 2009.

[9] P. W. Wypych and D. B. Hastie, "Theoretical modelling of rotary valve air leakage for pneumatic conveying systems," in *9th Asian Pacific Confederation Chemical Engineering Congress and Chemeca*, Christchurch, New Zealand, 2002.

[10] M. Utri, S. Höckenkamp, and A. Brümmer, "Fluid flow through male rotor housing clearances of dry running screw machines using dimensionless numbers," *IOP Conference Series: Materials Science and Engineering*, vol. 425, no. 1, pp. 1–12, 2018.

[11] M. Utri and A. Brümmer, "Fluid flow through front clearances of dry running screw machines using dimensionless numbers," in *International Conference on Screw Machines 2018, IOP Conference Series: Materials Science and Engineering*, 2018.

[12] A. A. Kotlov, "Influence of suction port parameters on integral characteristics of screw-type compressor," *IOP Conference Series: Materials Science and Engineering*, vol. 425, no. 1, 2018.

[13] R. Andres, J. Hesse, F. Hetze, and D. Low, "Cfd simulation of a two stage twin screw compressor including leakage flows and comparison with experimental data," *IOP Conference Series: Materials Science and Engineering*, vol. 425, no. 1, 2018.

[14] X. Liang and W. Wu, "Theoretical and experimental studies on oil injected twin screw air compressor under unload conditions," *IOP Conference Series: Earth and Environmental Science*, vol. 252, no. 3, pp. 1–13, 2019.

[15] H. H. Patel and V. J. Lakhera, "A critical review of the experimental studies related to twin screw compressors," *Proceedings of the Institution of Mechanical Engineers, Part E: Journal of Process Mechanical Engineering*, vol. 234, no. 1, pp. 157–170, 2020.

[16] H. H. Patel and V. J. Lakhera, "Modelling of leakages in rotary twin-screw compressor,," in *IOP Conference Series: Materials Science and Engineering, 20th International Conference on Recent Innovations in Engineering and Technology*, vol. 1070, Erode, Tamilnadu, India, December 2020.

[17] H. H. Patel and V. J. Lakhera, "An experimental technique to simulate and measure leakages in twin-screw compressor," *Engineering Research Express*, vol. 3, no. 15024, pp. 1–17, 2021.

[18] V. Vodicka, V. Novotny, Z. Zeleny, J. Mascuch, and M. Kolovratnik, "Theoretical and experimental investigations on the radial and axial leakages within a rotary vane expander," *Energy*, vol. 189, no. 116097, pp. 1–12, 2019.

[19] B. C. Lee, T. Yanagisawa, M. Fukuta, and S. Choi, "A study on the leakage characteristics of tip seal mechanism in the scroll compressor," in *International Compressor Engineering Conference at Purdue University*, pp. 15–24, West Lafayette, Indiana, USA, 2002.

[20] B. Fragerli, "CO2 compressor development," in *Workshop Proceedings-CO2 Technology in Refrigeration, Heat Pump and Air Conditioning Systems*, pp. 295–318, Netherlands, 1997.

[21] G. H. Lee, "Performance simulation of scroll compressors," *Proceedings of the Institution of Mechanical Engineers, Part A: Journal of Power and Energy*, vol. 216, no. 2, pp. 169–180, 2002.

[22] J. Wang and T. Liu, "Leakage model of axial clearance and test of scroll compressors," *Journal of Shanghai Jiaotong University (Science)*, vol. 25, no. 4, pp. 531–537, 2020.

[23] B. Peng, S. Zhao, and Y. Li, "Thermodynamic model and experimental study of oil-free scroll compressor," *Journal of Physics: Conference Series*, vol. 916, no. 1, p. 12, 2017.

[24] D. İmamoğlu and Ö. Ertunç, "Analysis of tip leakage in external gear pump," in *9th International Automotive Technologies Congress, OTEKON*, pp. 621–630, Bursa, Turkey, 2018.

[25] A. R. A. Muhammad, *Rotordynamics of Twin Screw Pumps*, Texas A&M University, 2013.

[26] Q. Zhang, J. Feng, J. Wen, and X. Peng, "3D transient CFD modelling of a scroll-type hydrogen pump used in FCVs,"

International Journal of Hydrogen Energy, vol. 43, no. 41, pp. 19231–19241, 2018.

[27] Q. Zhang, J. Feng, J. Wen, and X. Peng, "Study on the scroll compressors used in the air and hydrogen cycles of FCVs by CFD modeling," in *International Compressor Engineering Conference at Purdue University*, pp. 1–9, China, 2018.

[28] G. Singh, S. Sun, A. Kovacevic, Q. Li, and C. Bruecker, "Transient flow analysis in a Roots blower: experimental and numerical investigations," *Mechanical Systems and Signal Processing*, vol. 134, pp. 1–21, 2019.

[29] D. Ziviani, I. Bell, M. De Paepe, and M. Van Den Broek, "Comprehensive model of a single screw expander for ORC-systems," in *International Compressor Engineering Conference at Purdue University*, pp. 1–10, Belgium, 2014.

[30] D. Ziviani, A. Suman, J. Gabrielloni, M. Pinelli, M. D. E. Paepe, and M. Van Den Broek, "CFD approaches applied to a single-screw expander," in *International Compressor Engineering, Refrigeration and Air Conditioning, and High Performance Buildings Conferences*, pp. 1–10, Belgium, 2016.

[31] K. Kauder and R. Sachs, "Gas flow through gaps in screw-type machines," *VDI Berichte*, vol. 1715, pp. 83–98, 2002.

[32] R. Sachs, *A Thesis - Experimentelle Untersuchung von Gasströmungen in Schraubenmaschinen*, Dortmund University, 2002.

[33] A. J. C. Saint Venant and L. Wantzel, "Memory and experiments on air flow," *Journal de l'École Polytechnique*, vol. 16, no. Series 1, p. 85, 1839.

[34] ISO, *ISO 1217: 2009(E) - Displacement compressors- acceptance tests*, 2009.

[35] ISO, *ISO 5168:2005 Measurement of fluid flow — procedures for the evaluation of uncertainties,*, 2005.